

Adaptive Optics Imaging and Spectroscopy of Cygnus A: I. Evidence for a Minor Merger¹

Gabriela Canalizo², Claire Max^{2,3}, David Whysong⁴, Robert Antonucci⁴, Scott E. Dahm⁵

ABSTRACT

We present Keck II adaptive optics near infrared imaging and spectroscopic observations of the central regions of the powerful radio galaxy Cygnus A. The $0''.05$ resolution images clearly show an unresolved nucleus between two spectacular ionization/scattering cones. We report the discovery of a relatively bright ($K' \sim 19$) secondary point source $0''.4$ or 400 pc in projection southwest of the radio nucleus. The object is also visible in archival *Hubble Space Telescope* optical images, although it is easily confused with the underlying structure of the host. Although the near infrared colors of this secondary point source are roughly consistent with those of an L-dwarf, its spectrum and optical-to-infrared spectral energy distribution (SED) virtually rule out the possibility that it may be any foreground projected object. We conclude that the secondary point source is likely to be an extragalactic object associated with Cygnus A. We consider several interpretations of the nature of this object, including: a young star cluster peering through the dust at the edge of one of the ionization cones; an older, large globular cluster; a compact cloud of dust or electrons that is acting as a mirror of the hidden active nucleus; and the dense core of a gas stripped satellite galaxy that is merging with the giant elliptical host. The data presented here are most consistent with the minor merger scenario. The spectra and SED of the object suggest that it may be a densely packed conglomeration of older stars heavily extinguished by dust, and its high luminosity and compact nature are consistent with those of a satellite that has been stripped to its tidal radius. Further spectroscopic observations are nevertheless necessary to confirm this possibility.

¹Based on observations with the NASA/ESA Hubble Space Telescope, obtained from the data archive at the Space Telescope Science Institute. STScI is operated by the Association of Universities for Research in Astronomy, Inc. under NASA contract No. NAS 5-26555.

²Institute of Geophysics and Planetary Physics, Lawrence Livermore National Laboratory, 7000 East Avenue, L413, Livermore, CA 94550

³Center for Adaptive Optics, University of California, Santa Cruz, Santa Cruz, CA 95060

⁴Physics Department, University of California, Santa Barbara, CA 93106

⁵Institute for Astronomy, University of Hawaii, 2680 Woodlawn Drive, Honolulu, HI 96822

Subject headings: galaxies: active — galaxies: infrared — galaxies: interactions — galaxies: evolution — instrumentation: adaptive optics — galaxies: individual (Cygnus A)

1. Introduction

Mergers and strong interactions of galaxies are often cited as important triggering mechanisms for activity in radio galaxies. Many powerful radio galaxies exhibit dramatic signs of interactions (*e.g.*, Heckman et al. 1986; Smith & Heckman 1989; Ridgway & Stockton 1997), but many others appear to reside in early type galaxies that show no signs of interaction (*e.g.*, Dunlop et al. 2003). One interesting alternative is that, at least in some active nuclei, the fueling may be driven by minor mergers (Taniguchi 1999, and references therein). Signs of tidal interaction in these minor mergers would be more elusive, and their detection may require deep, high resolution observations attainable only with the *Hubble Space Telescope* (*HST*) and, at ground-based facilities, with the use of adaptive optics (AO).

The prototype radio galaxy Cygnus A is a Fanaroff-Riley class II radio galaxy showing two lobes extending to more than 60 kpc on either side of a giant, seemingly non-interacting (though gas rich and star-forming) elliptical host. Because of its proximity ($z = 0.056$) and extreme characteristics, Cygnus A has played a fundamental role in the study of virtually every aspect of powerful radio galaxies (see Carilli & Barthel 1996, for a review). Different lines of evidence indicate that Cygnus A harbors a heavily extincted quasar (*e.g.*, Ogle et al. 1997; Antonucci, Hurt & Kinney 1994). However, the giant elliptical shows an $r^{1/4}$ radial surface brightness profile (*e.g.*, Stockton, Ridgway & Lily 1994) and no large scale tidal features indicative of a recent merger event that might have triggered the nuclear activity.

We have obtained near infrared Keck II AO images of Cygnus A of unprecedented resolution ($\sim 0''.05$ or 50 pc for $H_0 = 70 \text{ km s}^{-1} \text{ Mpc}^{-1}$, assumed throughout the paper) and depth which reveal new exciting information. In this paper, we report on the discovery of a secondary point source in the central regions of Cygnus A, which may be the smoking gun of a minor merger event. In a subsequent paper (Canalizo et al., in preparation; hereafter Paper II) we discuss the spectroscopy of the nucleus, the morphology of the central regions, and the interpretation of our observations in the context of unified models.

2. Observations and Data Reduction

Near infrared spectroscopic and imaging observations of the central regions of Cygnus A were carried out using the Keck II AO system (Wizinowich et al. 2000a,b; Johansson et al. 2000) with the NIRC-2 camera (PI: K. Matthews & T. Soifer). The Keck II AO system is located on an optical bench at the Nasmyth platform of the 10-m telescope. The Xinetics deformable mirror has 349 degrees of freedom, of which approximately 249 are illuminated at any given time as the hexagonal pupil of the telescope rotates on the round deformable mirror. The Shack-Hartmann wavefront sensor is based on a 64×64 pixel Lincoln Laboratories CCD with read noise of approximately 6 electrons per pixel. The real-time computer is based on the Mercury RACE architecture, and uses sixteen Intel i860 floating-point CPUs. The control system's closed-loop bandwidth is typically about 30 Hz using natural guide stars ($V \lesssim 13.5$) as a wavefront reference. For the spectroscopic and imaging observations of Cygnus A, we guided on a $V \sim 13$ magnitude star $29'.4$ southwest of the nucleus. The sampling frequency of the wavefront sensor was 55 Hz.

Cygnus A was imaged in K' on UT 26 May 2002 through the NIRC-2 narrow field camera, which yields a plate scale of $0''.01 \text{ pixel}^{-1}$. The total integration time was 5×300 s, and the FWHM of stars near Cygnus A was $0''.05$. Imaging in J - and H -bands was done on UT 27 May 2002 through the wide field camera, yielding a plate scale of $0''.04 \text{ pixel}^{-1}$; total integration times were 6×60 s in J and 10×60 s in H . The FWHM in these images ranged from $0''.07$ near the guide star (GS) to $0''.1$ near Cygnus A in H -band, and from $0''.09$ to $0''.14$ in J -band. All the observations were obtained under photometric conditions. Standard stars from Persson et al. (1998) were observed throughout each night.

Spectroscopic observations in K' and J bands were obtained with NIRC-2 on UT 4 and 5 August 2002 respectively, using the wide field camera ($0''.04 \text{ pixel}^{-1}$) and the low resolution (LOWRES) grism. The width of the slit was $0''.08$, projecting to 2 pixels and yielding a resolution of 32 \AA per resolution element (2 pix) for the K' spectrum, and 20 \AA per resolution element for the J spectrum ($R \sim 700$ in each case). Total integration times were 2×1200 s for K' and 2×900 s for J . The choice of slit position angle was constrained by a number of limitations. Since the GS was nearly $30''$ away from Cygnus A, close to the limit for the steering mirrors, Cygnus A could only be positioned at certain places on the detector, and at certain angles that would maximize the possible distance between the steering mirrors and the GS. We chose a PA that would allow us to place the object in a region of the detector that would maximize the wavelength coverage, but that would at the same time minimize the flux contamination from the surrounding emission. The resulting slit PA was 140° . Nearby B8 and A0 stars were observed immediately after each science observation and used for telluric correction and flux calibration. These stars were also imaged through

J and K' filters and calibrated against photometric standards from Persson et al. (1998).

The spectra were reduced with IRAF, using standard reduction procedures. After correcting for dark current and bad pixels, flat fielding, and subtracting sky, we calibrated the 2-d spectrum in wavelength using the OH sky lines. We rectified the spectra by tracing the spectrum of a bright standard placed at the same position along the slit as the science target. The extracted science spectra were then corrected for atmospheric absorption using telluric standards.

3. A Secondary Point Source in the Core of Cygnus A

Figure 1 shows a NIRC-2 AO K' image of the central $8'' \times 8''$ region of Cygnus A. The unresolved nucleus is clearly seen between two spectacular ionization/scattering cones. As noted above, we postpone our analysis of these and other features in the central regions of Cygnus A to Paper II. However, on the suggestion of the referee, we provide a few remarks on the cones in Section 4.

In addition to the ionization cones, we find a bright secondary point source $\sim 0'.4$ or ~ 400 pc (in projection) west-southwest of the nucleus. What is the nature of this object? While the image is suggestive of a double nucleus in Cygnus A, we must consider all possibilities. First, it is conceivable that this object may be a faint foreground star in our Galaxy, particularly since Cygnus A is near the plane of the Galaxy ($b = 5.76^\circ$).

3.1. Secondary Point Source: a Projected Galactic Object?

The first step in investigating whether the secondary point source is a foreground object is to obtain its photometric colors and compare them to those of different galactic objects. Obtaining accurate photometry in AO images is challenging because of the difficulty in determining the point spread function (PSF). We attempted to obtain a suitable PSF that would account for anisoplanatism by observing pairs of stars where the GS had the same magnitude, position angle, and separation from the PSF as the GS used for Cygnus A. However, both the atmosphere and the performance of the AO system change rapidly between exposures, so it was not possible to obtain a good PSF using this method. Ideally, using a large aperture including most of the halo of the PSF would yield the most accurate photometry in AO imaging. It is obviously impossible to do this in the case of the secondary point source, since the object has a bright and highly structured background.

In order to circumvent these difficulties, we used as PSFs field stars from each image of

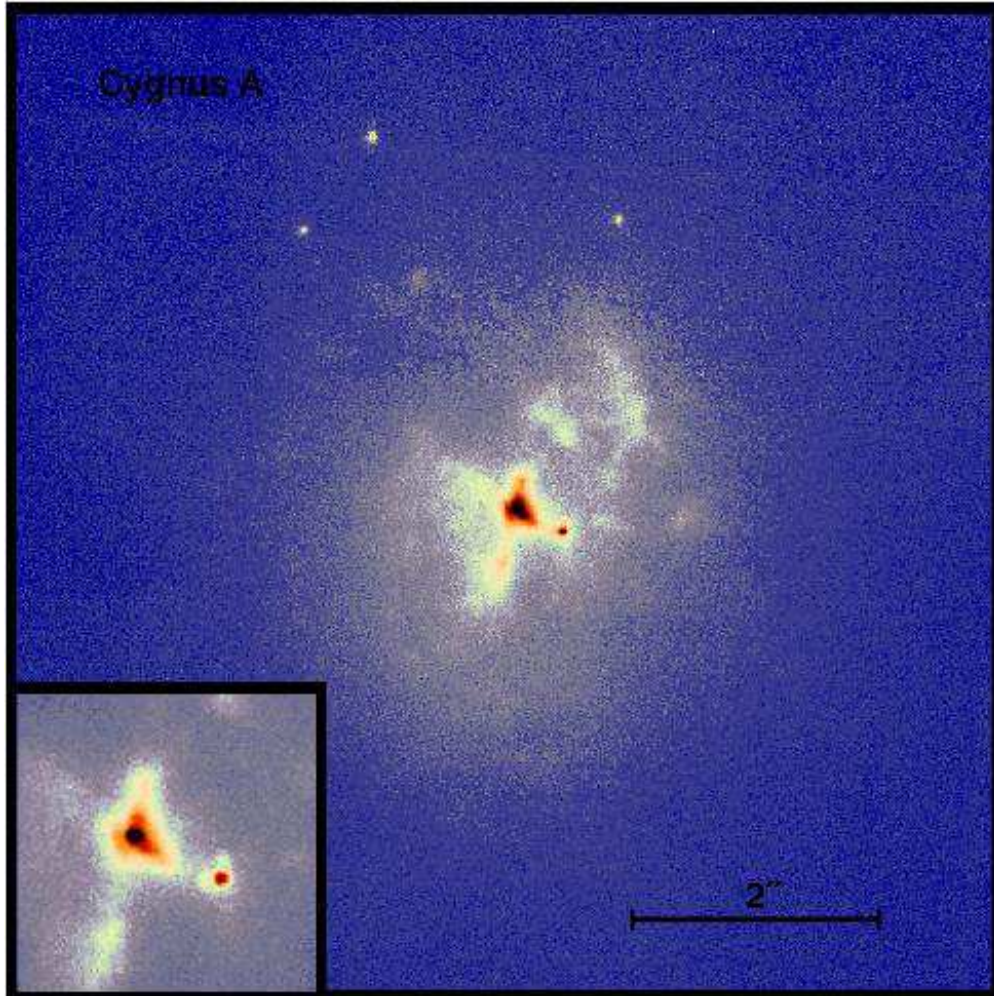


Fig. 1.— False color NIRC-2 AO K' image of the core of Cygnus A. In this and the following images North is up and East is to the left. The inset is $1''.3 \times 1''.3$ and shows the central region at a lower contrast to show the point-like nucleus as well as a secondary point source $0''.4$ to the west-southwest.

Cygnus A. We chose two stars at the same PA from the GS as the core of Cygnus A, one closer and the other farther away, to account for the effects of anisoplanatism. The stars were only a few arcseconds from Cygnus A and there was some contamination from the outskirts of the galaxy. We subtracted this contamination by fitting a low order polynomial to the background. We then calibrated these stars against standard stars by using a large (80 pixels) aperture. Next, we scaled the stars to match the secondary point source, and subtracted them. Finally, we used the scaling factor to obtain the flux of the secondary point source. We obtained consistent results using either PSF star. In order to further test the consistency of the method, we measured photometry of other stars in the field in this way and compared it with large aperture photometry; in every case, we obtained magnitudes consistent within 0.02 mag, even in the J image, where anisoplanatism is more significant.

The main source of uncertainty was determining the best PSF subtraction, since faint PSF residuals could be easily confused with the highly structured background underlying the secondary point source. In every case we achieved good fits to the point source, apparently leaving no residuals. However, we chose to estimate uncertainties by considering scaling factors that lead to obvious over- and undersubtractions of PSFs. The errors we quote as 1σ should then be regarded as very conservative.

We used the same method to measure photometry of the nucleus, obtaining larger errors since the background is more confused by the bright underlying structure. We list in Table 1 the photometry of the nucleus and that of the secondary point source, as well as their colors transformed to the CIT system (Persson et al. 1998). These magnitudes have not been corrected for Galactic extinction ($A_V=1.263$ towards Cygnus A; Schlegel et al. 1998), since we are making no assumptions as yet about the actual position or nature of the object. The K' flux we obtain for the nucleus is nearly a factor of two lower than the $2.25\ \mu\text{m}$ flux measured by Tadhunter et al. (1999), and nearly 10 times lower than the K -band flux measured by Djorgovski et al. (1991). This is not surprising since, due to the lower resolution in the HST and ground-based images, both of these measurements are expected to have more contamination from the bright structure underlying the nucleus. If, for example, we measure the flux of the nucleus in our K' AO images using a $0''.1$ aperture, we obtain a flux nearly identical to that measured by Tadhunter et al. (1999) in the HST images. This point, and the fact that the nucleus is well fitted by a point source, will be discussed in more detail in Paper II.

Table 1. Photometry of Cyg A Nucleus and Secondary Point Source

	2nd Pt. Source	Nucleus
V	25.03 ± 0.31	...
m_{F622W}	25.42 ± 0.17	...
I_C	23.41 ± 0.14	...
J	20.61 ± 0.11	21.15 ± 0.21
H	19.98 ± 0.12	20.42 ± 0.15
K'	19.14 ± 0.08	18.50 ± 0.14
$(J - H)_{\text{CIT}}^{\text{a}}$	0.62 ± 0.23	0.71 ± 0.35
$(H - K)_{\text{CIT}}^{\text{a}}$	0.82 ± 0.21	1.87 ± 0.29

^aTransformation to the CIT system using equations given by Persson et al. (1998) and assuming $K = K'$

In Fig. 2 we show the position of the secondary point source in the near infrared (NIR) color-color diagram. Also shown are the main sequence, dwarf and giant branches as given by Tokunaga (2000). Very low mass objects are also plotted: L-dwarfs from Dahn et al. (2002) and Kirkpatrick et al. (2000), and T-dwarfs from Dahn et al. (2002) and Burgasser et al. (2002). Figure 2 shows that the NIR colors of the secondary point source can only be consistent with a somewhat unusual L-dwarf if the object is a foreground star. If any amount of Galactic reddening is taken into account, the object is moved even farther away from the L-dwarf locus. Pre-main sequence (PMS) stars can also occupy this region of the diagram. However, PMS objects are always associated with star forming regions, and there are no such regions near the position of Cygnus A. Data from Two Micron All Sky Survey (2MASS) shows that a relatively small number of faint galaxies also fall in this region (see, *e.g.*, Jarrett et al. 2000); we will return to this possibility in section 3.2 when we consider different extragalactic objects.

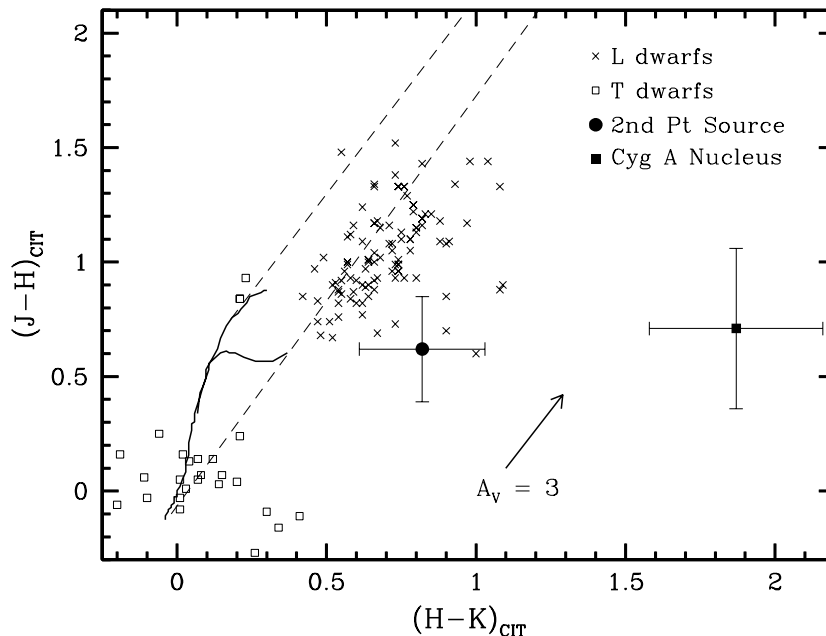


Fig. 2.— Color-color near infrared diagram in the CIT photometric system. The solid traces mark the main sequence (O9 through M6; lower branch) and giants (G0 through M7 upper branch). Dashed lines indicate the direction of galactic reddening, and a galactic reddening of $A_V=3$ is indicated by the arrow. L-dwarfs are plotted as crosses, and T-dwarfs as open squares. The secondary point source is plotted as a solid circle, and the nucleus of Cygnus A is plotted as a solid square.

An unabsorbed L-dwarf with $(J-K)_{CIT} = 1.42$ would be expected to have an absolute

magnitude M_J roughly between 11 and 13.5 (Dahn et al. 2002), which in turn would indicate that, if this object were an L-dwarf, it would be located at a distance of 200–800 pc. The object is visible in *HST* WFPC2 images (see below) and the first of these images was taken almost six years prior to our NIRC-2 image. We measure no displacement in six years. The proper motion of this object is then less than $6.6 \times 10^{-3} \text{ '' yr}^{-1}$, implying a tangential velocity of less than 6 km s^{-1} if the object were at 200 pc, or 25 km s^{-1} if it were at 800 pc. Although the implied velocity is somewhat lower than those expected for disk stars and those found for other L-dwarfs (*e.g.*, $\langle V_{tan} \rangle = 31 \pm 4 \text{ km s}^{-1}$ in Dahn et al. 2002) we cannot, on this basis alone, rule out the possibility that the object may indeed be an L-dwarf.

Through careful astrometry, we were able to identify the secondary point source in archival *HST* WFPC2 images. Figure 3 shows a three-color composite optical image of Cygnus A (left panel), where red corresponds to F814W, green to F622W, and blue to F555W (individual images first appeared in Jackson, Tadhunter & Sparks 1998; Jackson et al. 1996). We also show in the central panel of Fig. 3 a three-color near infrared image from our NIRC-2 data, where red is K' , green is H , and blue is J . The narrow field camera K' image is included on the right panel at the same scale for reference.



Fig. 3.— Three-color WFPC2 PC1 (left panel) and Keck NIRC-2 (central panel) images of the core of Cygnus A. For the WFPC2 PC1 image, red is the F814W filter, green is F622W, and blue is F555W. For the Keck NIRC-2 image, red is K' , green is H , and blue is J . A K' image is shown (in false color, right panel) for reference. Each image is $5''.9 \times 5''.9$.

We have used the position measured from our narrow field camera K' AO image (Fig. 1) to obtain optical photometry by fitting a PSF to the secondary point source in the WFPC2 images. For consistency, we used the same fitting method and PSF stars that we used for the NIR AO data. The resulting photometry is listed in Table 1. The optical spectral energy distribution (SED) of this object is bluer than those of L-dwarfs. In Fig. 4 we show an $I_C - J$

vs. $V - I_C$ diagram where we plot M- and L-dwarfs from Dahn et al. (2002) (T-dwarfs are off this diagram since their $V - I$ values are much larger). The secondary point source is clearly set apart at shorter wavelengths from these Galactic low mass objects. Therefore, based on its photometry, we conclude that it is highly unlikely that the secondary point source in Cygnus A is a foreground Galactic object.

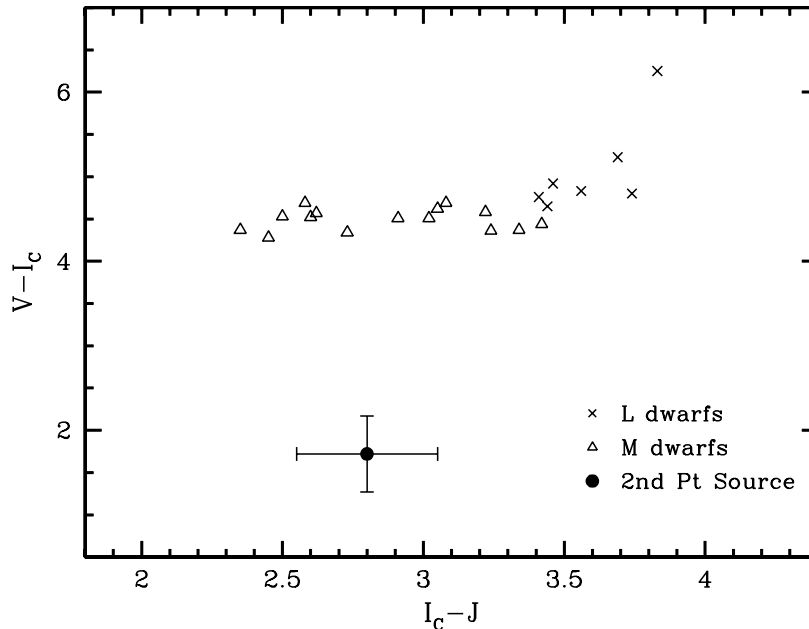


Fig. 4.— Color-color diagram in the CIT and Cousins photometric systems. L-dwarfs are plotted as crosses, and M-dwarfs as open triangles. The 1σ errors in the colors for these objects are typically smaller than the size of their symbols. The secondary point source is plotted as a solid circle, showing that the SED of this object is too blue to be an L-dwarf.

The reader will notice that the composite color *HST* image in Fig. 3 shows a very red object west of the secondary point source. This object appears so red because it is not visible in either the F622W or the F555W images. The F814W image was taken on UT 1996 April 8, roughly 2 and 1.5 years after the the first two were obtained. The red object is therefore very likely a supernova (SN) that went off some time after the first two sets of images were taken. We measure an absolute I magnitude $M_I = -15.43 \pm 0.09$ (correcting for Galactic reddening, but neglecting the k correction, which should be smaller than 0.1 magnitude). This magnitude is typical of a Type I or II SN that is roughly between 50 and 120 days old (Wheeler & Benetti 2000). The next set of *HST* observations of Cygnus A was obtained with NICMOS on UT 1997 December 15 (Tadhunter et al. 1999, 2000), when the SN was

~ 700 days old and would be at least 8 magnitudes fainter, which is why it is not visible in the 1997 NICMOS images. It is not possible to determine whether this is a type I or II SN based on this image alone. Type Ia SNe are believed to be the only type of SN occurring in quiescent elliptical galaxies (van den Bergh & Tammann 1991), presumably because older stellar populations dominate these galaxies. They may also be common near (and possibly triggered by) radio jets (Capetti 2002). However, the host galaxy of Cygnus A is known to have regions of star formation (*e.g.*, Fosbury et al. 1999; Jackson, Tadhunter & Sparks 1998; Stockton, Ridgway & Lily 1994), so this SN could potentially be a type II SN.

3.2. Secondary Point Source as an Extragalactic Object

If the secondary point source is not a projected Galactic object, then it is likely to be an extragalactic object associated with Cygnus A. A background galaxy would be virtually undetectable in the highly extinguished central regions of Cygnus A, unless the extinction is extremely patchy. The bright and compact nature of the secondary point source might suggest that it may be a massive young star cluster in the host galaxy of Cygnus A. It is conceivable that many such clusters could be present in the circumnuclear regions of Cygnus A, deeply obscured by dust. In this scenario, the secondary point source would be visible due to its strategic location near the edge of the cone, where the extinction might be less severe.

The K' spectrum (Fig. 5) shows a $\sim 5\sigma$ (per resolution element) continuum at the position of the secondary point source, with a spatial FWHM of $\sim 0''.08$, roughly consistent with the FWHM of $\sim 0''.07$ measured in the wide camera K' image obtained the same night. Similarly, the J -band spectrum shows a $\sim 3\sigma$ continuum. It is difficult to determine whether there are emission lines intrinsic to the secondary point source, as there is much extended emission associated with the ionization cone around the object (Paper II). The K' spectrum shows strong emission lines, identified in Fig. 5; however, the (spatial) peak of the emission is centered 1.5 pix or $0''.06$ southeast of the continuum, and therefore appears to come from the edge of the ionization cone, which underlies the continuum object. The same is true for the J -band spectrum, which shows strong [Fe II] emission at $1.258 \mu\text{m}$. Therefore we cannot use these emission lines to measure a redshift for the secondary point source, although we also cannot rule out the possibility that the object may indeed have fainter emission lines at the same redshift. A young star cluster, however, would be expected to be embedded in gas. This gas would be ionized by the hot stars forming an H II region, and the spectrum would show strong emission lines associated with the continuum object.

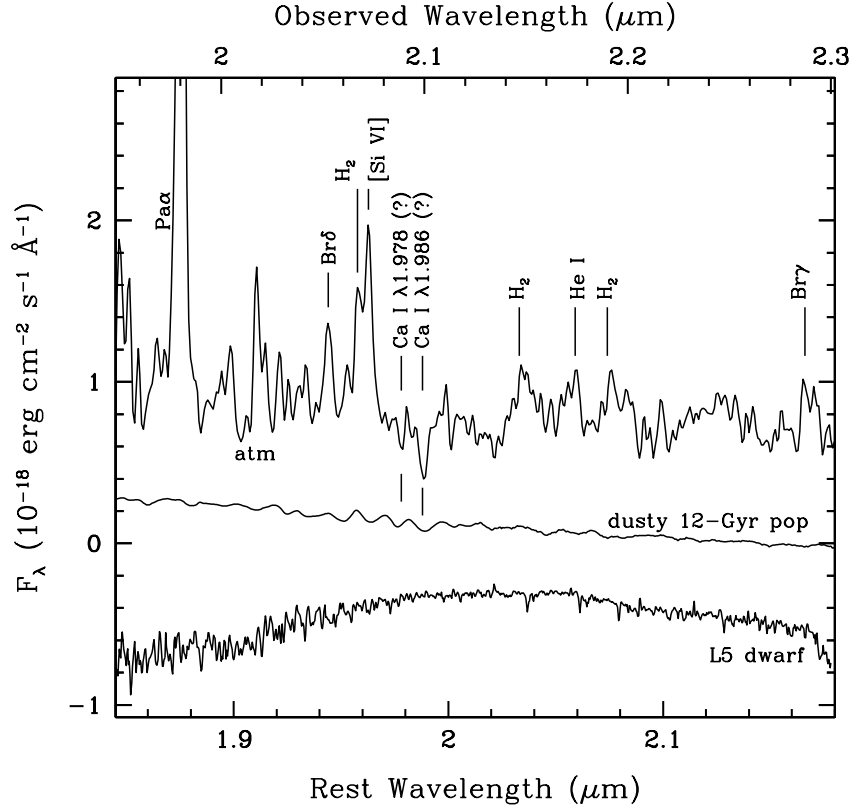


Fig. 5.— K' spectrum of secondary point source in Cygnus A (top trace). The top axis indicates the observed wavelength, and the bottom axis the rest frame wavelength, assuming $z = 0.056$. The spectrum has been smoothed using a gaussian of $\sigma = 1$ pixel. The strong emission lines come from the surrounding gas. The location of two possible absorption features is indicated. The middle trace is a reddened GISSSEL00 model (Bruzual & Charlot 2003) of a 12-Gyr old population at the redshift of Cygnus A (see text for details). The bottom trace is an L5 dwarf from McLean et al. (2001) plotted with respect to the top (observed wavelength) axis. The 12-Gyr old stellar population and the L5 dwarf spectra are normalized to match the flux of the secondary point source, and are shifted downward to allow for comparison.

The conspicuous absence of emitting gas in this object suggests that it may instead be a conglomeration of older stars. The signal to noise ratio of the spectrum of this $K'=19.1$ object is not high enough to allow us to identify unequivocally stellar absorption lines. In Fig. 5 we have plotted an isochrone synthesis model from the GISSEL00 empirical models (Bruzual & Charlot 2003). The model is a 12-Gyr old population at the redshift of Cygnus A ($z \sim 0.056$). We have also simulated the presence of embedded dust (which is obviously present in Cygnus A) by reddening the spectrum using the “dusty galaxy” models calculated by Witt, Thronson, & Capuano (1992). In these models, the dust and the stars are both assumed to have constant density within a sphere, and the only variable is the optical depth to the center at a specific wavelength; in this case we choose a V -band central optical depth of 6. While these models are highly artificial, they show the general nature of the reddening due to embedded dust. The final spectrum shows very roughly the same continuum shape as that of the secondary point source in Cygnus A, and two of the absorption features in the Ca I triplet (those at $1.978 \mu\text{m}$ and $1.986 \mu\text{m}$) are coincident with potential absorption features in the spectrum of the secondary point source (the third line, if present, is swamped by the extended [Si VI] emission). The 12-Gyr model is also a fair fit to the overall SED of the object (from V to K bands), except at J -band, where the flux of the model falls 2σ below the photometric point. Thus the spectrum could be consistent with a reddened older stellar population at the redshift of Cygnus A, but we will need deeper spectra to confirm the nature of this object.

A bright compact object formed by older stars could be a large globular cluster, although it seems unusual that we would not observe any other such clusters throughout the host galaxy. It is difficult to estimate the luminosity of the secondary point source since we do not know how much extinction there is at this point. But even without taking into account any extinction in Cygnus A, the secondary point source has an absolute K magnitude of $M_K = -17.92$. This is almost 500 times more luminous than the most luminous globular cluster in our Galaxy, ω Centauri (NGC 5139 Harris 1996), which has an $M_K = -10.22$, and ~ 4000 times more luminous than the average globular cluster in our Galaxy. Therefore, if the secondary point source in Cygnus A is indeed a conglomeration of older stars, it must be significantly more massive than a typical globular cluster. However, given its apparent size ($\lesssim 50$ pc), it must have similar or higher densities than a globular cluster.

Such conditions (*i.e.*, a large, densely packed group of older stars) can be found in the cores of low luminosity galaxies. At least in the case of ellipticals, low luminosity galaxies have much denser central regions than their high luminosity counterparts (see, *e.g.*, Faber et al. 1997). For example, a galaxy initially having one tenth the mass of the Cygnus A host would have a space density 20 times higher than that of the host at a radius of 1 pc, while a galaxy with a 1:100 mass ratio would have a 1:51 density ratio at the same radius

(Holley-Bockelmann & Richstone 1999). Kendall, Magorrian & Pringle (2003) investigate the dynamics of minor mergers for active galactic nuclei and estimate the mass loss of an infalling satellite simulated by a Hernquist sphere (see their equation 6). This estimate is simply obtained by equating the mean density of the satellite within its tidal radius to the mean density of the galaxy within the radius given by the distance between the satellite and the center of the primary galaxy. In the simulation, the satellite is truncated to its tidal radius and the density structure internal to this point remains unchanged. Although this assumption is unphysical, Kendall, Magorrian & Pringle (2003) argue that it is a reasonable approximation since the satellite will react to the density truncation on an internal dynamical timescale which is of the order of the orbital timescale. Following their method, we estimate the mass loss due to tidal stripping for satellites of different mass ratios with respect to Cygnus A. We simulate the Cygnus A host galaxy using the Sérsic density profile as given by Lima Neto, Gerbal & Márquez (1999) in their equation 17, with $\nu = 0.25$ and $p = 0.851$, which correspond to a de Vaucouleurs profile. We use the galaxy parameters for Cygnus A given by Marconi & Hunt (2003), so that $M_{bul} = 1.6 \times 10^{12} M_{\odot}$, $R_{eff} = 31$ kpc, and $\rho_o = 3.09 \times 10^3 M_{\odot} \text{ pc}^{-3}$. For satellites, we scale this density profile to match the parameters given by Marconi & Hunt (2003) for NGC 3115, NGC 4742, and M 32, which have mass ratios of 1:9, 1:145, and 1:1667 respectively, with respect to the Cygnus A host. We find that the 1:9 satellite loses $\sim 94\%$ of its mass by the time it reaches a distance of 400 pc to the nucleus; its remaining mass in the tidally stripped core is roughly 7×10^{-3} that of the host. Similarly, the 1:145 satellite loses $\sim 95\%$ of its mass and the remaining mass ratio is $\sim 4 \times 10^{-4}$ with respect to the host. Because of its much higher central density, the 1:1667 satellite only loses $\sim 60\%$ of its mass, and the resulting mass ratio is 2.4×10^{-4} . Simulating the satellites with Hernquist spheres scaled to match their observed parameters leads to similar results, within a factor of 2.

For comparison, we measure an H -band absolute magnitude for the Cygnus A giant elliptical host galaxy of $M_H \sim -25.2$, roughly consistent with the $M_R = -23.7$ measured by Carilli et al. (1989) (transformed to our choice of Cosmology), if the host has an SED typical of ellipticals (we use H rather than K' since our wide field H -band image is deeper). Neglecting the effects of extinction and assuming a similar mass to light ratio in the host and the putative merging galaxy, the latter would have roughly 6×10^{-4} the mass of the host. This is comparable to the mass ratios we obtain for the tidally stripped 1:145 and 1:1667 companions at a distance of 400 pc from the center of Cygnus A. All of these are obviously gross approximations and oversimplified assumptions, and they should only serve to provide some reference for the scales that we are discussing, and to show that the interpretation of the secondary point source as an infalling satellite is not unreasonable. Cygnus A is associated with a rich cluster of galaxies (possibly of Abell richness class 3; Owen et al. 1997). Thus

a merger between the giant elliptical host and a galaxy having a mass 100 or 1000 times smaller should not be an unlikely event.

The secondary point source in Cygnus A may then be the gas stripped core of a merging galaxy which has thus far survived a merger event. Holley-Bockelmann & Richstone (2000) consider the effects of a central massive black hole in the merger between an elliptical galaxy and a smaller satellite of higher density. They determine that the black hole can exert significant tidal forces and disrupt the core of the secondary during the final pericenter passes. During previous passes, however, the secondary will simply be stripped to its tidal radius and the core will remain intact since its density is greater than that of the primary anywhere (see also Merritt & Cruz 2001, for similar results from simulations including a black hole in the satellite). The satellite will survive even longer in high angular momentum encounters (*i.e.*, those with low eccentricity orbits). Kendall, Magorrian & Pringle (2003) find that low angular momentum encounters are more efficient in delivering material to the central regions of the primary. If the putative minor merger in Cygnus A is responsible for the triggering of the nuclear activity, we may be witnessing a more radial encounter after the first few pericenter passes or a few $\times 10^7$ yr. This timescale could be consistent with the age estimate (lower limit based on synchrotron aging arguments) for the radio source in Cygnus A of $10^{6.8}$ yr (Carilli & Barthel 1996, and references therein).

One last (unlikely) possibility is that the secondary point source is rather reflected light from a cloud with a direct view of the hidden quasar. There are several known cases in which a fairly isolated off-nuclear cloud has been shown to be dust scattering light from a hidden nucleus, and even electron-scattering “mirrors” are seen off of the nucleus in some cases. Particularly instructive is the case of PKS 2152–69, shown to be highly polarized by di Serego Alighieri et al. (1988) and convincingly argued by them to be dust-reflected light from a hidden AGN. One piece of evidence was the extraordinary “blueness” of the spot. The secondary point source in Cygnus A certainly appears to be bluer than the nucleus (see Figs. 2 and 3), but this could be due to different amounts of extinction towards each one of these objects, dust emission, and the fact that the nuclear K' photometry has a large contribution from strong emission lines (Paper II).

Several tests can in principle be made of this hypothesis for the secondary point source in Cygnus A. High polarization, perpendicular to the radius vector from the nucleus, would be quite persuasive. We examined the *HST* NICMOS polarization images, originally taken by Tadhunter et al. (2000). However, the marginal spatial resolution, presence of bright nearby structure, and low signal-to-noise ratio prevented a reliable measurement.

A second test is a check for broad emission lines in the putative scattered nuclear spectrum. For this test it helps to know in advance the width of the broad emission lines,

and this raises a complication. The broad Mg II line width is $\sim 7,500 \text{ km sec}^{-1}$, according to Antonucci, Hurt & Kinney (1994). These authors argued that the line was scattered into the line of sight by dust, though spectropolarimetry was not obtained at that wavelength. That aperture was, however, placed over what appears in the optical range as the SE (continuum-emitting) “nucleus”. Later Ogle et al. (1997) found an extremely broad H α (FWHM = $26,000 \text{ km sec}^{-1}$) line in polarized flux. Because the ratio of the total flux in this line to Mg II is relatively small, and because the width was so much larger, the simplest picture was that the H α line is scattered by electrons.

For the secondary point source, assuming a line width of $7,500 \text{ km s}^{-1}$ FWHM, we estimate that any broad Pa α line can have no more than $\sim 90 \text{ \AA}$ equivalent width as measured from our spectrum (Fig. 5). The limited broad Pa α equivalent width measurements reported in the literature are much higher, in the range between 200 and 500 \AA (*e.g.*, Courvoisier, Bouchet & Robson 1992; Kollatschny & Fricke 1983). This argues against the dust-mirror hypothesis. Our equivalent width limit on any emission line with FWHM = $26,000 \text{ km s}^{-1}$ like the H α line in polarized flux (Ogle et al. 1997) is not constraining, but such an isolated and localized electron-scattering mirror seems unlikely.

Finally, one can consider the reasonableness of the putative scattered flux given the solid angle subtended by the secondary as seen from the primary. The secondary has a size $\lesssim 0''.05$ and a distance from the primary of $0''.4$ in projection. Thus it is likely to subtend no more than $\sim 1/60$ steradians, or $\sim 0.13\%$ of the total sky as seen from the hidden nucleus. The νF_ν flux of the secondary point source at $2 \mu\text{m}$ is $(1.5 \times 10^{14} \text{ Hz})(\sim 15 \mu\text{Jy}) = \sim 2.2 \times 10^{-14} \text{ erg sec}^{-1}$. Now we need the intrinsic value of νF_ν at $2 \mu\text{m}$ from the primary for comparison. The $2 \mu\text{m}$ emission is likely to be highly anisotropic, given its high scattering polarization (Tadhunter et al. 2000). Instead, we use the nuclear value of νF_ν at $12 \mu\text{m}$ of $\sim 120 \text{ mJy}$ (Whysong & Antonucci 2001; Radomski et al. 2002) or $\nu F_\nu = 9 \times 10^{-11} \text{ erg sec}^{-1}$, which should be more isotropic. To the present level of accuracy, we can assume the same value to apply to the expected $2 \mu\text{m}$ νF_ν brightness of the hidden quasar, so the hotspot has of order 2×10^{-4} times the flux of the hidden nucleus at $2 \mu\text{m}$. (Here we have assumed unit dust albedo; this is conservative because we are trying to see whether we can rule out sufficient dust reflection for the secondary point source. Also, deviations from unity (*e.g.*, Draine 2003, Fig. 9) are smaller than geometrical uncertainties in this argument.) This is consistent with the mirror interpretation, but the argument would be far more telling if a gross conflict were shown.

4. Brief Remarks on the Cones

As mentioned above, apparent edge-brightened “cones” are clearly detected in our images (Figs. 1 and 3). Tadhunter et al. (1999) refer to an “edge-brightened bicone” in their 2.0 μm *HST* images of Cygnus A (see also Jackson, Tadhunter & Sparks 1998, for a description of the cones in the optical). An analogy is made there to young stellar object morphologies and this analogy can be extended to the η Carinae nebula called the Homunculus. Similarities exist in both the total-flux and the polarization images, and in all cases these objects can be described, to first order, as bipolar reflection nebulae.

Our impression is that in some cases the scattered light is seen more clearly in the near-IR than in the optical/UV, because the former wavelengths are less affected by foreground “weather” in the form of dusty gas of modest optical depth. This is seen for example in NGC 1068, in which the far-side scattering cone is only clear in the near-IR (Packham et al. 1997). Antonucci & Barvainis (1990) argued that this is also the case for 3C223.1 and for Cen A. There are other objects however in which UV dust scattering in extended merger debris provides the clearest scattered-light picture of bicones (Hurt et al. 1999).

The edge-brightening in Cygnus A and other objects is likely to result in general from a nonuniform distribution of ambient material (see, *e.g.*, Balsara & Krolik 1993, Sec. 5, for a physical explanation). However, a remarkable peculiarity of Cygnus A itself is that, while the total-flux morphology is symmetric about the cone axis, the polarized flux is not (Tadhunter et al. 2000). The edge of the bicone on which the secondary point source lies has somewhat less total flux and much less polarization than the other edge. The secondary point source may thus provide a clue to the different natures of the two bicone edges. We will discuss this further in Paper II (and Kishimoto et al., in preparation, for HST ultraviolet imaging polarimetry of this object).

The bicone morphology also begs the question of the role of Cygnus A in the subject of hidden quasars inside radio galaxies. Most or even all of the highest-luminosity subset of FR II narrow-line radio galaxies have hidden quasars, as shown by polarimetric and other arguments. By contrast radio galaxies on the lower end of the radio luminosity function seem to be heterogeneous with respect to possession of such a (visible or hidden) “thermal” optical/UV continuum source (*e.g.*, Whysong & Antonucci 2001; Antonucci 2002; Meisenheimer et al. 2001). Thus Cygnus A is expected to have a hidden quasar. This is strongly suggested by the bicone morphology, and confirmed by the quasar spectrum observed in scattered light with spectropolarimetry (Ogle et al. 1997)

The exceptional clarity of the apparent cone edges, along with constraints on the inclination angle, would seem to make our measured opening angle intelligible in the context

of the torus opening angle. However, such an inference would be premature because of the *HST* polarimetric evidence cited above (Tadhunter et al. 2000) that the cone edges differ fundamentally in character despite the evident reflection symmetry in the total flux images. Thus we postpone any interpretation of the bicone to Paper II.

5. Summary

Our high resolution, deep Keck II AO images of Cygnus A show a secondary point source in the central regions of Cygnus A. We have considered different possibilities in attempting to determine the nature of this object. The SED and NIR spectrum of the object are inconsistent with those of foreground Galactic objects. The most likely explanation is that it is indeed an object associated with Cygnus A.

The absence of ionized gas obviously associated with the object is inconsistent with it being a star forming region, and its high luminosity is orders of magnitude greater than that expected for a globular cluster. The object has a spectrum and colors that are distinct from those of the underlying structure; hence, it does not appear to be a bright compact region of the scattering cone which is seen as a discrete object due to patchy obscuration. Finally, the upper limits we place on the presence of broad $\text{Pa}\alpha$ in the spectrum are inconsistent with a dust mirror interpretation.

We are left with the possibility that the secondary point source in Cygnus A may be the tidally stripped core of a lower mass galaxy that is merging with the giant elliptical. The spectrum of the object is roughly (though not exclusively) consistent with that of a dusty compact object made of older stars. The observed luminosity is consistent with that of a satellite that has lost most of its mass as it is being accreted, and the observed size ($\lesssim 50$ pc) is consistent with that of an object that has been stripped to its tidal radius.

The interpretation of a merging low luminosity companion is appealing as it would seem to fit in with several observed properties in Cygnus A. First, this minor merger could have provided the means to fuel the black hole, resulting in the nuclear activity that we observe in Cygnus A. At least the rough dynamical timescales seem to be consistent with the estimates for the timescale of the radio source (both in the order of 10^7 yr). The merger event could have also triggered the central starburst in Cygnus A that has been suggested by *HST* (Fosbury et al. 1999; Jackson, Tadhunter & Sparks 1998) and ground-based imaging and spectroscopy (Stockton, Ridgway & Lily 1994). The gas dynamics in the host of Cygnus A show a peculiar structure with discontinuities, velocity reversals, and double components akin to the structure found in nearby merger remnants (Stockton, Ridgway & Lily 1994).

The apparent counter-rotating gas in the nuclear regions is most easily explained as a result of a merger event. Cygnus A also shows dust lanes which are roughly perpendicular to the radio jets (see Fig. 3). A large fraction of radio galaxies show similarly oriented dust lanes (Verdoes Kleijn et al. 2000) and these are thought to be debris trails of minor mergers (Kendall, Magorrian & Pringle 2003). The jets would then be roughly perpendicular to the orbit of the encounter that triggered the nuclear activity. Cygnus A would fit this scenario, as the putative merging companion appears to be near the plane of the dust lanes.

However plausible this scenario may seem, it remains highly speculative at this point. A deeper AO spectrum showing clearly the presence of absorption lines will allow us to determine the precise nature and dynamics of this object. Failing to find absorption lines in the spectrum, we will need to obtain high angular resolution polarimetry to test the hypothesis that the secondary point source is a mirror of the hidden quasar. If, however, the secondary point source is confirmed to be a merging companion, it will be of great interest to model the encounter in detail, and Cygnus A will provide, yet again, the testbed to study important phenomena relevant to powerful active galaxies.

We gratefully acknowledge Mark Lacy, Alan Stockton, Luis Ho, Makoto Kishimoto, and Bruce Macintosh for helpful discussions. We thank Ian McLean and his collaborators for providing us with their NIRSPEC spectra of L and T dwarfs, and Stephane Charlot for allowing us to use the GISSEL00 models prior to publication. We also thank the anonymous referee for helpful suggestions. Data presented herein were obtained at the W.M. Keck Observatory, which is operated as a scientific partnership among the California Institute of Technology, the University of California and the National Aeronautics and Space Administration. The Observatory was made possible by the generous financial support of the W.M. Keck Foundation. R.A.’s research is partially supported by NSF grant AST-0098719. This work was supported in part by the National Science Foundation Science and Technology Center for Adaptive Optics, managed by the University of California at Santa Cruz under cooperative agreement No. AST-9876783. This work was supported in part under the auspices of the U.S. Department of Energy, National Nuclear Security Administration by the University of California, Lawrence Livermore National Laboratory under contract No. W-7405-Eng-48.

REFERENCES

- Antonucci, R. 2002, in “Astrophysical Spectropolarimetry”, eds. Trujillo-Bueno, F., Moreno-Inseris, and F. Sánchez, Cambridge, UK: Cambridge University Press
- Antonucci, R., & Barvainis, R. 1990, *ApJ*, 363, L17

- Antonucci, R., Hurt, T., Kinney, A. 1994, *Nature*, 371, 313
- Balsara, D. S., & Krolik, J. H. 1993, *ApJ*, 402, 109
- Bruzual, G., Charlot, S., 2003, *MNRAS*, submitted
- Burgasser, A. J., Kirkpatrick, J. D., Brown, M. E., Reid, I. N., Burrows, A., Liebert, J., Matthews, K., Gizis, J. E., Dahn, C. C., Monet, D. G., Cutri, R. M., Skrutskie, M. F. 2002, *ApJ*, 564, 421
- Capetti, A. 2002, *ApJ*, 574, L25
- Carilli, C. L., Dreher, J. W., Conner, S., & Perley, R. A. 1989, *AJ*, 98, 513
- Carilli, C. L., & Barthel, P. D. 1996, *A&ARv*, 7, 1
- Courvoisier, T. J.-L., Bouchet, P., Robson, E. I. 1992, *A&A*, 258, 272
- Dahn, C. C. et al. 2002, *ApJ*, 124, 1170
- di Serego Alighieri, S., Courvoisier, T. J.-L., Fosbury, R. A. E., Tadhunter, C. N., Binette, L. 1988, *Nature*, 334, 591
- Djorgovski, S., Weir, N., Matthews, K., Graham, J. R. 1991, 367, L67
- Draine, B. T. 2003 *ARAA*, 41, in press [astro-ph/0304489]
- Dunlop J. S., McLure, R. J., Kukulka, M. J., Baum, S. A., O’Dea, C. P., Hughes, D. H. 2003, *MNRAS*, 340, 1095
- Faber, S. M. et al. 1997, *AJ*, 114, 1771
- Fosbury, R. A. E., Vernet, J., Villar-Martn, M., Cohen, M. H., Ogle, P. M., Tran, H. D. 1999, in *The Most Distant Radio Galaxies*, ed. H. J. A. Rottgering, P. N. Best, and M. D. Lehnert., (Amsterdam: Royal Netherlands Acad.), 311
- Harris, W. E. 1996, *AJ*, 112, 1487
- Heckman, T. M., Smith, E. P., Baum, S. A., van Breugel, W. J. M., Miley, G. K., Illingworth, G. D., Bothun, G. D., & Balick, B. 1986, *ApJ*, 311, 526
- Holley-Bockelmann, K., & Richstone, D. O. 2000, *ApJ*, 517, 92
- Holley-Bockelmann, K., & Richstone, D. O. 2000, *ApJ*, 531, 232

- Hurt, T., Antonucci, R., Cohen, R., Kinney, A., Krolik, J., 1999, *ApJ*, 514, 579
- Jackson, N., Tadhunter, C., Sparks, W. B., Miley, G. K., Macchetto, F. 1996, *A&A*, 307, L29
- Jackson, N., Tadhunter, C., Sparks, W. B. 1998, *MNRAS*, 301, 131
- Jarrett, T. H., Chester, T., Cutri, R., Schneider, S., Skrutskie, M., Huchra, J. P. 2000, *AJ*, 119, 2498
- Johansson, E. K., Acton, D. S., An, J. R., Avicola, K., Beeman, B. V., Brase, J. M., Carrano, C. J., Gathright, J., Gavel, D. T., Hurd, R. L., Lai, O., Lupton, W., Macintosh, B. A., Max, C. E., Olivier, S. S., Shelton, J. C., Stomski, P. J., Tsubota, K., Waltjen, K. E., Watson, J. A., and Wizinowich, P. L. 2000, *Proc. SPIE* 4007, 600.
- Kendall, P., Magorrian, J., & Pringle, J. E. 2003, *MNRAS*, in press [astro-ph/0305079]
- Kirkpatrick, J. D., Reid, I. N., Liebert, J., Gizis, J. E., Burgasser, A. J., Monet, D. G., Dahn, C. C., Nelson, B., Williams, R. J. 2000, *AJ*, 120, 447
- Kollatschny, W., & Fricke, K. J., 1983, *A&A*, 122, 33
- Lima Neto, G. B., Gerbal, D., Márquez, I. 1999, *MNRAS*, 309, 481
- Marconi, A. & Hunt, L. K. 2003, *ApJ*, 589, L21
- Meisenheimer, K., Haas, M., Müller, S. A. H., Chini, R., Klaas, U., Lemke, D. 2001, *A&A*, 372, 719
- Merritt, D. & Cruz, F. 2001, *ApJ*, 551, L41
- McLean, I. S., Prato, L., Kim, S. S., Wilcox, M. K., Kirkpatrick, J. D., Burgasser, A. 2001, *ApJ*, 561, L115
- Ogle, P., Cohen, M., Miller, J. S., Tran, H. D., Fosbury, R. A. E., Goodrich, R. W. 1997, *ApJ*, 482, L37
- Owen, F. N., Ledlow, M. J., Morrison, G. E., Hill, J. M. 1997, *ApJ*, 488, L15
- Packham, C., Young, S., Hough, J. H., Axon, D. J., Bailey, J. A. 1997, *MNRAS*, 288, 375.
- Persson, S. E., Murphy, D. C., Krzeminski, W., Roth, M., & Rieke, M. J. 1998, *AJ*, 116, 2475

- Radomski, J. T., Pia, R. K., Packham, C., Telesco, C. M., Tadhunter, C. N. 2002, *ApJ*, 566, 675
- Ridgway, S. E. & Stockton, A. 1997, *AJ*, 114, 511
- Schlegel, D. J., Finkbeiner, D. P., Davis, M. 1998, *ApJ*, 500, 525
- Smith, E. P. & Heckman, T. M. 1989, *ApJ*, 341, 658
- Stockton, A, Ridgway, S. E. & Lily, S. 1994, *AJ*, 108, 414
- Tadhunter, C. N., Packham, C., Axon, D. J., Jackson, N. J., Hough, J. H., Robinson, A., Young, S., Sparks, W., 1999 *ApJ*, 512, 91
- Tadhunter, C. N., Sparks, W., Axon, D. J., Bergeron, L., Jackson, N. J., Packham, C., Hough, J. H., Robinson, A., Young, S. 2000, *MNRAS*, 313, 52
- Taniguchi, Y. 1999, *ApJ*, 524, 65
- Tokunaga, A. T. 2000 in *Astrophysical Quantities, Fourth Edition*, ed. A. Cox (New York, Springer-Verlag), Chapter 7
- van den Bergh, S., Tammann, G. A. 1991, *ARAA*, 29, 363
- Verdoes Kleijn, G. A., de Zeeuw, P. T., Baum S. A., O’Dea, C. P., van der Marel, R. P., Xu, C., Carollo, C. M., Noel-Storr, J. 2000, in *Galaxies and their Constituents at the Highest Angular Resolutions*, eds. R. Schilizzi, S. Vogel, F. Paresce, M. Elvis, Manchester UK, August 2000
- Wheeler, J. C., & Benetti, S. 2000 *Astrophysical Quantities, Fourth Edition*, ed. A. Cox (New York, Springer-Verlag), Chapter 18
- Whysong, D., & Antonucci, R. 2001, *ApJ*, submitted [astro-ph/0106381]
- Witt, A. N., Thronson, H. A., & Capuano, J. M. 1992, *ApJ*, 393, 611
- Wizinowich, P., Acton, D. S., Shelton, C., Stomski, P., Gathright, J., Ho, K., Lupton, W., Tsubota, K., Lai, O., Max, C., Brase, J., An, J., Avicola, K., Olivier, S., Gavel, D., Macintosh, B., Ghez, A., Larkin, J. 2000a, *PASP*112, 315
- Wizinowich, P. L., Acton, D. S., Lai, O., Gathright, J., Lupton, W., and Stomski, P. J. 2000b, *Proc. SPIE* 4007, 2